World's first microscale infrared thermal image of 25-mm-diameter, ~3500-m-deep subsurface tight rocks: Overestimated brittleness jeopardizes China's deep energy revolution

Shuheng Du[1,2,*] and Zhuoshen Zong[1,2]

[1]State Key Laboratory of Nonlinear Mechanics, Institute of Mechanics, Chinese Academy of Sciences, Beijing 100190, China
[2]School of Engineering Science, University of Chinese Academy of Sciences, Beijing 100049, China
*Correspondence: dushuheng@imech.ac.cn

Received: September 28, 2025; Accepted: March 30, 2026; Published Online: April 8, 2026; https://doi.org/10.59717/j.xinn-geo.2026.100220

Citation: Du S. and Zong Z. (2026). World's first microscale infrared thermal image of 25-mm-diameter, ~3500-m-deep subsurface tight rocks: Overestimated brittleness jeopardizes China's deep energy revolution. *The Innovation Geoscience* **4**:100220.

Dear Editor,

Ensuring energy security has long been a fundamental challenge for human survival. In the 21st century, despite rapid advances in new energy technologies, geological energy (oil, gas, and geothermal energy) remains the cornerstone of the global energy mix. With shallow geological resources largely depleted, the deep Earth has become a core target for energy exploration, marking the entry of energy development into the deep and unconventional resources era.[1,2,3]

The United States achieved a successful shale gas revolution in the early 21st century via horizontal drilling and hydraulic fracturing technologies. However, despite vast resource endowments, China's deep and unconventional energy revolution faces formidable challenges.[4] Deep oil, gas, and geothermal resources are hosted in deep tight rocks, whose effective development hinges on fracturing. As the target of fracturing operations, rock brittleness is the primary determinant of rock fracturability.

Accurate rock brittleness evaluation is critical to engineering safety and energy security. Fracturing incidents occur frequently worldwide; engineering failures stemming from inaccurate brittleness evaluation waste massive time, labor, and material resources, leading to irreparable losses.

EXISTING ROCK BRITTLENESS EVALUATION METHODS: ADVANTAGES OF MINERALOGICAL APPROACHES

Most deep reservoir rocks in China feature strong compositional heterogeneity, making their accurate and efficient characterization both essential and highly challenging. Current rock brittleness evaluation methods are mainly divided into two categories: mechanical methods and mineralogical methods.[5,6]

Mineralogical methods are rooted in the material basis of brittleness and avoid "phenomenon dependence". Rock brittleness is essentially the macroscopic manifestation of the mechanical behavior of its constituent minerals. Rocks with a higher proportion of rigid minerals (e.g., quartz, feldspar) are more prone to brittle fracture, whereas those enriched in plastic minerals (e.g., mica, clay minerals) tend to exhibit ductile deformation.

The core logic of mineralogical methods is to quantify brittleness directly via metrics linked to mineral composition (e.g., brittle mineral content, brittle-plastic mineral ratio), giving this approach clear and traceable physical meaning.

In complex deep high-temperature and high-pressure (HTHP) environments, mechanical simulation experiments are extremely challenging and costly, and suffer from a strong "size effect". In contrast, mineralogical methods are lower-cost, more efficient, and deliver more stable, reproducible results.

We therefore posit that mineralogical methods have unique advantages in large-scale application, universality, and compatibility with geological mechanisms, making them the preferred approach for rock brittleness evaluation—with irreplaceable value in resource exploration and engineering geology.

LIMITATIONS OF TRADITIONAL MINERALOGICAL METHODS: FIELD PRACTICE CONTRADICTIONS

However, traditional mineralogical methods are not universally applicable. Field practices in the Junggar Basin, Ordos Basin, and other regions in western China show that many "high-quality brittle layers" identified by these methods fail to generate the expected large-scale fracture networks, with both fracturing efficiency and energy production far below predictions—a long-standing puzzle for researchers and engineers.

To resolve this fundamental issue, we must re-examine traditional mineral-driven brittleness evaluation and quantify the contribution of individual minerals to brittleness from a new dimension.

NOVEL METHODOLOGY: MICROSCALE INFRARED THERMOGRAPHY AND EXPERIMENTAL DESIGN

To this end, we introduce macro-lens infrared thermography,[7,8] and present the world's first microscale thermal image of a 25-mm-diameter, ~3500-m-deep subsurface tight rock sample.

In a strictly temperature-controlled environment, we set a uniform emissivity (ε) of 1. This is not a mere equation simplification, but an innovative experimental design: complex mineral assemblages and states in deep rocks preclude individual emissivity calibration, and this uniform setting provides "thermal fingerprints" for mineral/state differentiation, fulfilling the core requirement of resolving compositional and textural differences. Based on the Stefan-Boltzmann Law:

$$M = \sigma \varepsilon T^4 \tag{1}$$

With $\varepsilon = 1$, we derive:$M = \sigma T_{app}^4$ .Where M is the total radiant exitance; σ is the Stefan-Boltzmann constant; $\varepsilon$is emissivity; T is the true temperature of the i-th feldspar grain; T_{app} is the apparent temperature of the i-th feldspar grain (in Kelvin, K), used as a proxy for grain weathering degree.

We define T_{app} by Equation (2):

$$T_{app} = \left(\frac{M}{\sigma}\right)^{\frac{1}{4}} \tag{2}$$

EXPERIMENTAL FINDINGS: WEATHERING-INDUCED FELDSPAR BRITTLENESS DETERIORATION

We selected deep tight oil-bearing conglomerates from Xinjiang, China.[7] Those samples from subsurface HTHP reservoirs have non-negligible feldspar content, with highly variable weathering degrees across individual feldspar grains. Notably, all samples are classified as "high-quality brittle layers" by the traditional Mineral Brittleness Index (*MBI*), yet their actual field fracturing performance varies significantly.

We conducted the world's first comparative experiment with fully synchronized field-of-view apparent temperature measurement and automated mineralogical identification. Three strict controls were implemented for temperature measurement: (1) a constant-temperature chamber to eliminate ambient temperature fluctuations; (2) a blackbody-calibrated infrared camera with a fixed measurement distance to avoid radiation attenuation; (3) five repeated measurements per sample, with a relative error < 3% to ensure data stability.

Our results reveal a critical finding: clay-altered feldspar exhibits significantly lower T_{app} than unweathered feldspar, driven by enhanced heat dissipation from its microporous structure (Figure 1). Calibration against TIMA automated mineral identification results from 20 representative samples

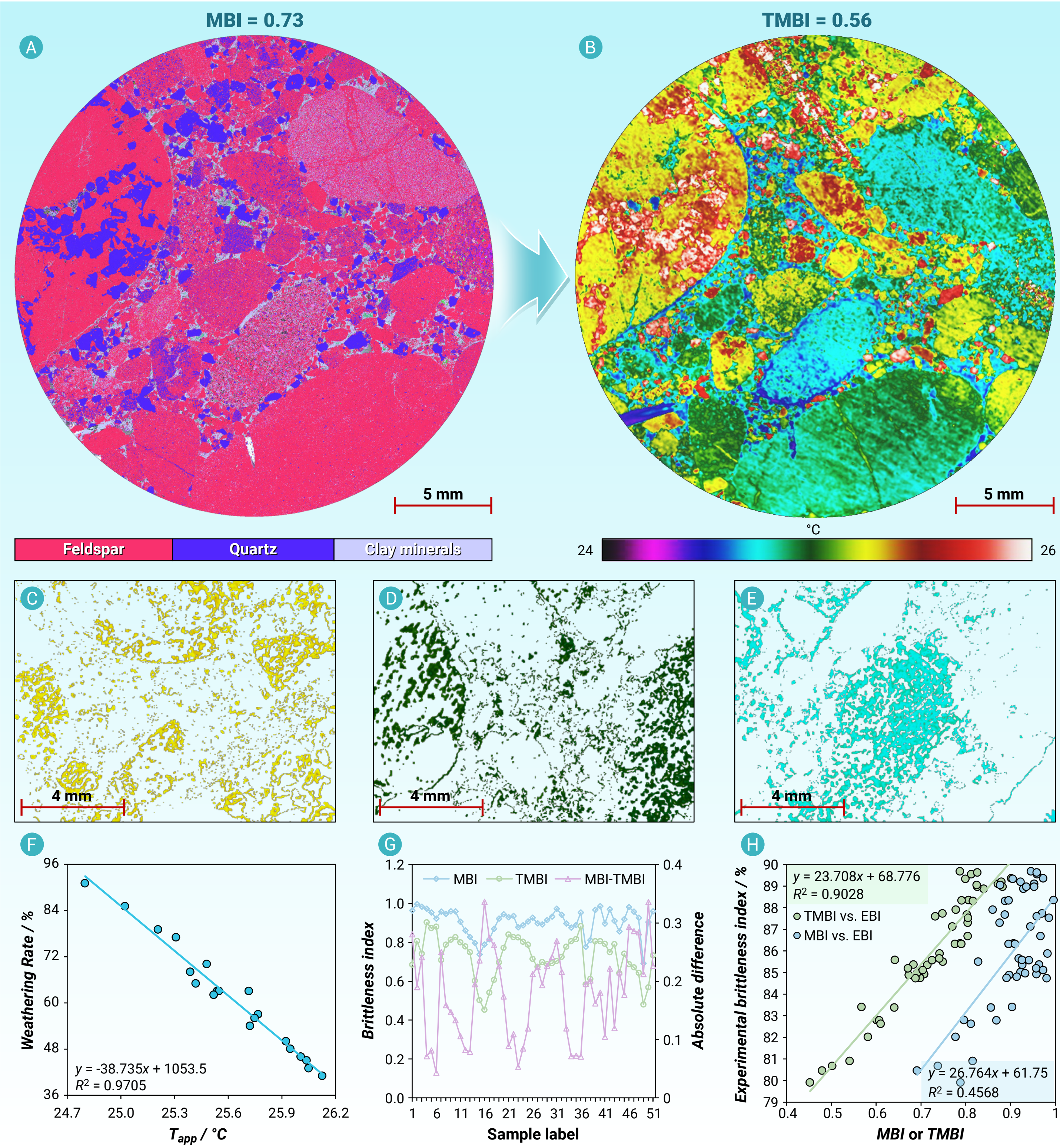

Figure 1. Comprehensive interpretation of the microscale thermal image of the 25 mm-diameter deep subsurface rock (A) Mineral composition distribution map of deep oil-bearing tight conglomerates based on TIMA automated mineralogy. (B) Corresponding world's first apparent temperature distribution map of the 25 mm-diameter rock sample, with extracted high, medium, and low apparent temperature regions, revealing low-weathering (C), moderate-weathering (D), and high-weathering feldspar (E), respectively. (F) Correlation between apparent temperature and feldspar weathering rate. (G) Variations in *MBI*, *TMBI*, and their absolute difference across samples. (H) Correlations of *TMBI* and *MBI* with the experimental brittleness index (*EBI*).

shows that infrared-measured T_{app} has a strong negative linear correlation with feldspar clay alteration rate (R^2 = 0.9705), enabling precise quantification of feldspar weathering degree (Figure 1F). The apparent temperature difference ΔT_{app} thus has a quantitative correlation with weathering rate (Equation 3):

$$Weathering\ rate \propto \left| T_{app} - T_{app}^{fresh} \right| \quad (3)$$

Where T_{app}^{fresh} is the reference temperature of unweathered feldspar.

This finding exposes a critical flaw in the traditional mineral-driven brittleness evaluation framework: it treats feldspar as a mechanically homogeneous phase and ignores the severe brittleness deterioration caused by chemical weathering.[9,10] This methodology is also theoretically applicable to other weatherable brittle minerals (e.g., carbonates), as carbonate dissolution forms porous networks analogous to feldspar clay alteration, which also modify thermal radiation properties; however, temperature thresholds must be recalibrated for carbonate systems (e.g., the full dissolution threshold of calcite requires dedicated measurement).

As shown in Figure 1, quartz remains largely stable during weathering, whereas feldspar readily forms clay-altered microdomains. While the mineral framework of altered feldspar is preserved, its interior is filled with clay minerals (predominantly illite-smectite mixed layers).

This "framework-sponge texture" severely impairs the mechanical integrity of feldspar. During fracturing, altered feldspar with this texture exhibits clay-like ductile behavior rather than the brittle response of pristine feldspar. However, existing models assign equal weight to unweathered and highly clay-altered feldspar, resulting in systematic deviations in brittleness prediction.

DEVELOPMENT OF THE THERMO-MINERAL BRITTLENESS INDEX (*TMBI*)

Based on this, we propose an apparent temperature weighting factor ω_i to calibrate the brittleness contribution of individual feldspar grains (Equation 4):

$$\omega_i = \frac{T_{\text{app},i} - T_{\text{app}}^{min}}{T_{\text{app}}^{max} - T_{\text{app}}^{min}} \tag{4}$$

Where ω_i is the apparent temperature weight factor for the *i*-th feldspar grain; $T_{\text{app},i}$ is the apparent temperature of the *i*-th feldspar grain (K), a proxy for grain weathering degree; T_{app}^{min} is the threshold temperature of fully weathered feldspar (K), corresponding to the "zero brittleness contribution" baseline; T_{app}^{max} is the reference temperature of unweathered feldspar (K), corresponding to the "fully brittle state" reference. The fully weathered threshold is determined via cross-validation with TIMA data (Figure 1A), using pure clay region temperatures as the baseline and iteratively adjusting to match TIMA-identified fully weathered feldspar domains.

The effective brittle content of feldspar $S_{\text{Fsp}}^{\text{eff}}$ is thus corrected as (Equation 5):

$$S_{\text{Fsp}}^{\text{eff}} = \left(\frac{\sum(\omega_i \cdot S_i)}{\sum S_i}\right) \cdot S_{\text{Fsp}} \tag{5}$$

Where $S_{\text{Fsp}}^{\text{eff}}$ is the effective brittle content of feldspar (%), representing the corrected net contribution of feldspar to rock brittleness; S_i is the area of the *i*-th feldspar grain (mm^2), reflecting the geometric weight of the grain; S_{Fsp} is the total areal content of feldspar (%), representing the total potential brittle mineral content.

Finally, we established the Thermo-Mineral Brittleness Index (TMBI) as (Equation 6):

$$TMBI = S_{\text{Qz}} + S_{\text{Fsp}}^{\text{eff}} \tag{6}$$

Where *TMBI* is the Thermo-Mineral Brittleness Index (%), characterizing the true brittleness of rocks (range: 0–100%); S_{Qz} is the areal content of quartz (%).

The core assumptions underpinning *TMBI* are: (1) weathering alters the thermal properties of minerals; (2) apparent temperature differences are dominated by weathering intensity; (3) feldspar (≥ 30% content) is the dominant brittle mineral in the target rock. Its applicable boundaries are: (1) suitable for deep tight reservoirs (depth > 3000 m, quartz- or feldspar-dominated); (2) not applicable to clay-rich (≥ 40%) or carbonate-dominated reservoirs without dedicated threshold recalibration.

IMPLICATIONS: CORRECTING BRITTLENESS OVERESTIMATION FOR CHINA'S DEEP ENERGY REVOLUTION

Comparative analysis of 51 representative samples from different depths of 5 wells in the study area reveals a significant quantitative discrepancy between traditional *MBI* and the proposed *TMBI*: the average absolute difference between the two indices is approximately 17%, with the difference increasing with weathering intensity. This demonstrates systematic overestimation of rock brittleness by *MBI* (Figure 1G), and explains the mediocre production performance of previously identified "high-quality brittle layers".

To validate *TMBI* accuracy, we obtained the Young's modulus and Poisson's ratio values of all 51 samples., calculating the Experimental Brittleness Index (*EBI*) from the normalized average of Young's modulus and Poisson's ratio (Figure 1H). Cross-plot analysis shows a strong positive correlation between *TMBI* and *EBI* (R^2 = 0.9028), whereas *MBI* exhibits only a weak correlation (R^2 = 0.4568). This confirms that *TMBI*, by accounting for feldspar weathering, far outperforms *MBI* in capturing the true mechanical brittleness of rocks, eliminates *MBI*'s overestimation bias, and provides a more robust basis for reservoir fracturing design.

Future work will expand the sample set to cover more regions, lithologies, and mineral types, and establish a direct correlation between *TMBI* and field fracturing performance. We conclude that widespread brittleness overestimation using traditional methods is subtly undermining the progress of China's deep energy revolution. Failure to recognize and correct this systematic bias will inevitably lead to greater waste of human and financial resources, jeopardizing China's overall energy security and thus requiring urgent attention.

REFERENCES

1. Hughes J. D. (2013). A reality check on the shale revolution. *Nature* **494**:307–308. DOI:10.1038/494307a
2. Thomas M., Partridge T., Harthorn B. H., et al. (2017). Deliberating the perceived risks, benefits, and societal implications of shale gas and oil extraction by hydraulic fracturing in the US and UK. *Nat. Energy* **2**:1–7. DOI:10.1038/nenergy.2017.54
3. Jolie E., Scott S., Faulds J., Chambefort I., et al. (2021). Geological controls on geothermal resources for power generation. *Nat. Rev. Earth Environ.* **2**:324–339. DOI:10.1038/s43017-021-00154-y
4. Atkinson G. M., Eaton D. W. andIgonin N. (2020). Developments in understanding seismicity triggered by hydraulic fracturing. *Nat. Rev. Earth Environ.* **1**:264–277. DOI:10.1038/s43017-020-0049-7
5. Meng F., Wong L. N. Y. and Zhou H. (2021). Rock brittleness indices and their applications to different fields of rock engineering: A review. *J. Rock Mech. Geotech. Eng.* **13**:221–247. DOI:10.1016/j.jrmge.2020.06.008
6. Bedford J. D., Faulkner D. R. and Lapusta, N. (2022). Fault rock heterogeneity can produce fault weakness and reduce fault stability. *Nat. Commun.* **13**:1–7. DOI:10.1038/s41467-022-27998-2
7. Du S., Zhao A. and Wei, Y. (2024). The dominant mineralogical triggers hindering the efficient development of the world's largest conglomerate oilfield. *Int. J. Hydrogen Energy* **60**:688–701. DOI:10.1016/j.ijhydene.2024.02.061
8. Trapp-Müller G., Caves Rugenstein J., Conley D. J., et al. (2025). Earth's silicate weathering continuum. *Nat. Geosci.* **18**:691–701. DOI:10.1038/s41561-025-01743-y
9. Du S., Bai L., Zhao A., et al. (2025). Infrared thermal imaging under a macro lens empowers geo-energy exploration and development: Application scenarios and scheme conceptions. *Adv. Geo-Energy Res.* **16**:4–7. DOI:10.46690/ager.2025.04.02
10. Okada T., Fukuhara T., Tanaka S., et al. (2020). Highly porous nature of a primitive asteroid revealed by thermal imaging. *Nature* **579**:518–522. DOI:10.1038/s41586-020-2102-6

FUNDING AND ACKNOWLEDGMENTS

This work was jointly supported by National Natural Science Foundation of China (No. 12241205), Youth Innovation Promotion Association CAS (No. 2023021)，Beijing Natural Science Foundation (No. 8232054) and Young Elite Scientists Sponsorship Program by CAST and BAST (No. YESS20220094 and No. BYESS2023182). The funders had no role in the study design, data collection and analysis, decision to publish, or preparation of the manuscript.

DECLARATION OF INTERESTS

The authors declare no competing interests.